Gene 860 (2023) 147245

Contents lists available at ScienceDirect

Gene

journal homepage: www.elsevier.com/locate/gene

Identification and molecular characterization of novel sucrose transporters in the hexaploid wheat (*Triticum aestivum* L.)

Depika Prasad [a,1], Woo Joo Jung [b,1], Yong Weon Seo [a,*]

[a] Department of Plant Biotechnology, Korea University, Seoul 02841, South Korea
[b] Institute of Life Science and Natural Resources, Korea University, Seoul 02841, South Korea

ARTICLE INFO

Edited by Kundan Kumar

Keywords:
Wheat
Sucrose transporters
Abiotic stress
Synteny

ABSTRACT

Common wheat (*Triticum aestivum*) is a major cereal crop grown and consumed globally. Recent advances in sequencing technology have facilitated the exploration of large and repetitive genomes. Plant sucrose transporter (*SUT*) genes are vital components of energy transport systems that play prominent roles in various plant functions, such as signaling and stress regulation. In this study, we identified and analyzed five novel sucrose transporter genes in wheat. The wheat sucrose transporter genes were divided into five clades based on their phylogenetic relationships. Synteny analysis revealed that synteny in the genome is highly conserved between wheat and rye, barley, and *Brachypodium*. Furthermore, the *cis*-element analysis indicated that sucrose transporter genes might be regulated by light and some phytohormone-related transcriptional factors. Overall, plant tissue-specific gene expression revealed enhanced expression of the transporter genes in the root and stem, whereas they were differentially expressed under abiotic stress treatments (cold, heat, NaCl, PEG-6000, and sucrose). These results indicate that each *TaSUT* gene may play a crucial role in stabilizing plants under stress by actively regulating the energy demands of cells. The findings of this study may provide a basis for further research on sucrose transporters and their significant roles in plant energy metabolism as well as in abiotic stress response, signaling, and regulation.

1. Introduction

Wheat is considered one of the most economical crops globally and is a major source of dietary carbohydrates. The larger size of the hexaploid wheat genome impedes the rapid progress in research. However, the gradually increasing availability of data has helped elucidate the comprehensive working mechanisms of wheat. The wheat genome is approximately 17 Gb, with each subgenome being approximately 5.5 Gb (Ling et al., 2018; Walkowiak et al., 2020). Unravelling the genes and genomes in wheat would facilitate the identification and manipulation of genes to obtain and augment the desired phenotypical traits.

In recent years, sucrose has gained much interest due to its diverse roles in metabolic functions, sensing, and plant development and transition stages (Jiang et al., 2015; Koch, 2004; Ruan, 2014). Sucrose is the primary form of photoassimilate that is translocated from the source to sink organs in plants (Stein and Granot, 2019). The active allocation of photoassimilates in the form of sucrose, from the source to the sink organs in plants, is mediated by sucrose transporters/carriers (SUT/SUC) (Deol et al., 2013). These transporters are currently being extensively studied in several plant species because sucrose distribution in plants depends on symplastic movement and transport across plasma membranes for intercellular transport, which is performed by sucrose transporters. Sucrose transporters belong to the major facilitator superfamily (MFS) and represent the largest group of secondary active membrane transporters (Niño-González et al., 2019). In *Arabidopsis*, nine sucrose transporters have been identified and investigated (Rottmann et al., 2018). Studies conducted with various plants, such as grapevines, tomatoes, *Arabidopsis*, and rice, have demonstrated that overexpression or the absence of sucrose transporters deter plant growth both vegetatively and reproductively (Cai et al., 2017; Dasgupta et al., 2014; Li et al., 2012; Reuscher et al., 2014; Zhang et al., 2010). However, only two *SUT* genes and their homologs have been currently identified in wheat

Abbreviations: ABA, Abscisic acid; MeJA, Methyljasmonate; PEG, polyethylene glycol; PCR, polymerase chain reaction; HMM, Hiddn Markov model; SUT, sucrose transporter.

* Corresponding author.
E-mail address: seoag@korea.ac.kr (Y.W. Seo).
[1] These authors contributed equally to this work.

https://doi.org/10.1016/j.gene.2023.147245
Received 13 September 2022; Received in revised form 2 January 2023; Accepted 27 January 2023
Available online 1 February 2023

(*Triticum aestivum* L.) (Aoki et al., 2002; Deol et al., 2013). Both studies identified each sucrose transporter gene and its copies along with the similarities and differences in the proteins. The two studies also showed the expression levels of *TaSUT1* and *TaSUT2* in tissues and observed the cellular localization of the proteins.

Moreover, research on various plants has revealed the diverse roles of sucrose transporters in addition to their primary role in sucrose transportation. Sucrose transporter 1 (*SUT1*) plays a crucial role in efficient phloem loading in maize, potato, tobacco, carrot, and *Arabidopsis* leaves (Baker et al., 2016; Burkle et al., 1998; Gottwald et al., 2000; Riesmeier et al., 1994; Shakya and Sturm, 1998; Slewinski et al., 2009). Similar functions have been identified in certain herbaceous plants (Oner-Sieben and Lohaus, 2014), sugar beets (Nieberl et al., 2017), and common beans (Santiago et al., 2020). *SUT1* overexpression in tobacco also affects plant survival and root elongation under aluminum stress (Kariya et al., 2017). Sucrose transporter 2 (SUT2) in maize contributes significantly to the vegetative growth of the plant as well as its agronomic yield, apart from remobilizing sucrose from the vacuoles for use in growing tissues (Leach et al., 2017). In *Arabidopsis*, SUT2 transports glucosides in addition to sucrose (Chandran et al., 2003), whereas overexpression of *SUT2* in tomato (Wang et al., 2016) and melon (Cheng et al., 2018) enhances the fruit sucrose content. The roles of *SUT2* also include the phosphorylation of targets in response to drought (Ma et al., 2019), and cold stress tolerance (Zhao et al., 2022). In addition to *SUT2*, *SUT3* plays a role in separating the phloem from the mesophyll and in a single, subepidermal cell layer of the carpels, which is vital for pod dehiscence and possibly in pod shatter (Meyer et al., 2000). It also plays critical roles in the sink and sources of the rubber biosynthesis pathway (Klaewklad et al., 2017), acts as a principal transporter for carbon delivery into secondary cell wall forming wood fibers (Mahboubi et al., 2013), and also affects pollen development, pollen germination, and pollen tube growth (Lemoine et al., 1999). Seed germination regulation in *Arabidopsis* (Li et al., 2012), plant growth and response to abiotic stress in sweet potatoes (Wang et al., 2020), mediating the circadian-regulated genes and ethylene production in potatoes (Chincinska et al., 2013), response to water stress and photosynthesis in Populus (Frost et al., 2012), regulation of fruit sugar accumulation in apples (Peng et al., 2020), and involvement in plant cell shape during mini protoplast culture, are some of the established functions of *SUT4*. *SUT5* appears to have a potential role in sink development and photoassimilate storage, *SUT6* may be a potential candidate for phloem loading during vegetative and reproductive growth in sorghum (Milne et al., 2013), and *SUT7* may engage in endosperm formation and grain filling in maize (Finegan et al., 2021).

The *SUT* family engages in a multitude of functions in various plants however, research is quite limited in wheat. Therefore, exploring the putative functional roles of sucrose transporter genes in wheat will help better understand the related metabolic pathways as well as create avenues for utilizing these genes to increase the quality and yield of crop production. Hence, we aimed to identify the *SUT* gene family using the recently published wheat reference genome and investigate the evolution and molecular functions of these genes. The *SUT* gene family in wheat and its closely related species were classified according to phylogenetic tree analysis. Their functions were observed through GFP-tagged subcellular localization and esculin uptake assays. Furthermore, tissue-specific gene expression and responses under diverse abiotic stress conditions are presented.

2. Materials & methods

2.1. Identification and sequence analysis of TaSUT genes

All published *SUT* genes in *Arabidopsis thaliana* were retrieved from the *Arabidopsis thaliana* database (https://www.arabidopsis.org/index.jsp). Using these genes as queries, a BLASTn search was performed to screen *SUT* genes expressed in wheat from the EnsemblPlants *Triticum aestivum* database (https://plants.ensembl.org/Triticum_aestivum/Info/Index). The genes with the highest BLAST scores and an e-value < 0.001 were identified as *SUT* homologs in wheat. The genes and their coding sequences (CDS) were obtained from the EnsemblPlants database, and the exon–intron structure was visualized via GSDS 2.0 (Hu et al., 2015). The conserved motif in each gene sequence was searched using the MEME Suite 5.5.0 (Timothy et al., 2015). The identified SUT proteins all belonged to SUT family according to InterProScan database search (https://www.ebi.ac.uk/interpro/search/sequence/), and the 3D structure of the proteins was predicted using the Phyre2 server (Kelley et al., 2015).

For chromosomal localization, the genomic sequence of each *SUT* gene was searched in the recently published wheat genome IWGSC RefSeq v2.1 (Zhu et al., 2021) to identify the location of each respective *SUT* gene on chromosomes. The length of wheat chromosomes and the start and the end position of the genes were retrieved from the database, and then the genes were localized on each wheat chromosome using the Advanced Circos tool in TBtools v1.098769 (Chen et al., 2020).

2.2. Phylogenetic tree and synteny analysis

SUT genes have also been identified in maize, rice, barley, *Brachypodium*, *Arabidopsis,* and wheat to identify patterns in the evolution of *SUT* genes in related species. Therefore, a phylogenetic tree was constructed to group related *SUT* genes. The phylogenetic tree was created using MEGA X software (Kumar et al., 2018) using the neighbor-joining method with the bootstrap 1000 based on the SUT amino acid sequence FASTA file from various species. The wheat SUT amino acid sequence FASTA file was run on Clustal Omega (https://www.ebi.ac.uk/Tools/msa/clustalo/), and multiple sequence alignment (MSA) was obtained. The alignment was visualized using the ESPript 3.0 (Robert and Gouet, 2014).

For synteny analysis of wheat *SUT* genes with closely related species, genome and gene annotation data were downloaded from the Ensembl Plants, Chinese National Genomics Data Center (https://bigd.big.ac.cn/), IPK Galaxy Blast Suite (https://galaxy-web.ipk-gatersleben.de/), and Phytozome 13 server (https://phytozome-next.jgi.doe.gov/) for wheat, rye, barley, and *Brachypodium*, respectively. Synteny analysis was performed using TBtools (Chen et al., 2020). Briefly, common gff, ctl, and collinearity files between two species were generated using the One Step MCScanX tool, and a synteny relationship was plotted using dual synteny plot TBtools.

2.3. Cis-acting element analysis

Promoters 1.5 kb upstream of the start codon of each *TaSUT* gene were identified from the EnsemblPlants database. The obtained promoter sequences were then used as queries to search for *cis*-elements using PlantCARE (Lescot et al., 2002) (https://bioinformatics.psb.ugent.be/webtools/plantcare/html/).

2.4. Gene cloning of TaSUT genes

To clone the *SUT* genes, gene-specific primers were designed from the 5′ and 3′ UTR of the obtained cDNA sequences (Table S2) using the NCBI Primer Blast (https://www.ncbi.nlm.nih.gov/tools/primer-blast/index.cgi?LINK_LOC=BlastHome). PCR was performed using the PrimeSTAR® GXL DNA Polymerase (Takara Bio Inc., Japan) with Korean "Keumgang" wheat cDNA as a template. Each gene was cloned into the pLUG-Prime® TA-cloning vector (iNtRON Biotechnology, Korea), and the sequence was verified using Sanger sequencing (Bionics Co., Korea).

2.5. GFP subcellular localization

To identify subcellular localization, the coding sequences of *TaSUT1*, *TaSUT2*, *TaSUT3*, *TaSUT4*, *TaSUT6*, and *TaSUT7* genes were cloned into

pCR™8/GW/TOPO®, and further subcloned into pMDC43 vectors using LR clonase (Thermo Fisher Scientific Inc., Waltham, MA, USA) to produce the GFP-TaSUT fusion protein. The vectors were transformed into *Agrobacterium tumefaciens* L. GV3101 using the freeze-thaw method (Chen et al., 1994) and introduced into the epidermal cells of the tobacco (*Nicotiana tabacum*) leaf. GFP fluorescence was visualized three days after infiltration and images were captured at 488 nm wavelength. Red chlorophyll auto-fluorescence was visualized at 555 nm wavelength using a confocal laser scanning microscope (CLSM) (Carl Zeiss, Germany).

2.6. Protoplast esculin uptake assay

A protoplast assay was performed to functionally characterize the novel *TaSUT* genes and analyze their transport activities, as outlined by Rottmann and Stadler (2019), with a few modifications to the protocol. One-week-old *T. aestivum* cv. Keumgang seedlings were used for protoplast isolation and transformation, whereas the pMDC43 vector construct was used for plasmid design. Following protoplast isolation and transfection, 10 μL esculin suspended in W5 buffer (0.9% NaCl, 125 mM $CaCl_2$, 5 mM KCl, 5 mM glucose, 1.5 mM MES, pH 5.7) was added. The tube was gently inverted to allow for homogenous mixing and incubated for 40 min at 25 ℃. After the protoplast settled at the bottom of the tube, the supernatant was removed and replaced with 300 μL of W5 buffer without esculin. Subsequently, 150 μL was transferred into an SPL confocal dish (200350) and visualized using CLSM. GFP and esculin fluorescence images were captured in sequential mode using a Zeiss confocal laser scanning microscope.

2.7. Plant growth and abiotic stress/phytohormone treatments

Thirty mature, dry seeds were germinated on moist germination paper (Anchor Paper Co., USA) at room temperature for six days. The germinated seedlings with even growth were then transplanted at nine seedlings each into a Magenta box (6.5 × 6.5 × 20 cm; Greenpia Technology Inc., Korea) containing polypropylene mesh and grown in 200 mL of half-strength Hoagland nutrient solution (H2395; Sigma-Aldrich, St. Louis, MO, USA). The seedlings were grown in a growth chamber under controlled conditions at 22/20 °C (day/night) with a 16/8h photoperiod. Hoagland's nutrient solution was replenished every two days. When the fourth leaf was visible, seedlings maintained in the chamber were subjected to abiotic stresses in triplicate at four different time intervals within the 24 h period. Drought 20% (PEG6000), cold (4 °C), heat (40 °C), osmotic (10% sucrose), and salt (200 mM NaCl) stress were induced in the growing seedlings, and samples were collected at 0, 6, 12, and 24 h, respectively. For phytohormone treatments, 1 mM of ABA (A8451; Sigma-Aldrich, St. Louis, MO, USA) and MeJA (392707; Sigma-Aldrich, St. Louis, MO, USA) were prepared in 0.1% Tween 20 solution and sprayed on the plant leaves. The samples were collected before and 24 h after the treatments. These samples were stored at −80 °C until used for RNA extraction.

2.8. Gene expression analysis

Total RNA was extracted from the total shoots of plants in the three-leaf stage using the NucleoZol reagent (MACHEREY-NAGEL, Germany), and the integrity was verified on an agarose gel stained with ethidium bromide. RNA purity was measured with the Colibri Microvolume Spectrophotometer (JC Bio, Korea). The Takara Prime Script™ 1st Strand cDNA synthesis kit (Takara, Japan) was used to synthesize cDNA from 1 μg of RNA, according to the manufacturer's instructions. Real-time PCR was conducted using the fluorescent DNA-intercalating dye SYBR Green (Applied Biological Materials Inc., Richmond, BC, Canada) on a CFX Connect Real-Time PCR detection system (Bio-Rad, USA). Each reaction was performed in biological triplicate, and actin was used as an endogenous control for template cDNA normalization. Fold changes were calculated using the $2^{-\Delta\Delta CT}$ method (Livak and Schmittgen, 2001). Statistical analysis was performed using the Microsoft Excel data analysis package. Differences in gene expression were evaluated using Student's *t*-test, and data are presented as means ± standard error. The statistical significance is denoted in the figures.

Wheat tissue-specific gene expression and during diurnal cycle were observed *in silico*. For the observation of tissue-specific gene expression, the primary gene ID was run in the Wheat Gene Expression Database of WheatOmics 1.0 (Ma et al., 2021), and the normalized expression value of each *TaSUT* gene was obtained. The expression values of each *TaSUT* gene from the roots, stems, leaves, spikes, and grains were obtained at various Zadoks scales. For the observation of gene expression during diurnal cycle, previously reported RNAseq data (Rees et al., 2022) were downloaded and gene expressions at ZT0, 4, 8, 12, 16, 20, and 24 were analyzed. Differential *TaSUT* expressions among wheat tissues and during diurnal cycle were plotted using Heatmapper (Babicki et al., 2016).

3. Results

3.1. Identification and phylogenetic analysis of SUT genes in Triticum aestivum

Seven *SUT* genes were identified in *Triticum aestivum*, among which *TaSUT1* and *TaSUT2* have already been investigated in wheat (Aoki et al., 2002; Deol et al., 2013). We identified five new *SUT* genes in wheat by investigating the wheat reference genome. Sequence alignment and a conserved domain search revealed that all *TaSUT* proteins belong to SUT family (Fig. 1). Homoeologs of *TaSUT1*, *TaSUT2* and *TaSUT3* genes shared more than 98% similarity, *TaSUT4* and *TaSUT5* genes shared over 91% similarities while *TaSUT6* and *TaSUT7* shared over 95% similarities. The 3D structure of TaSUT proteins also confirmed the presence of transporter domains. Each transporter possessed 11 or 12 transmembrane regions (Fig. 2B). The exon–intron structure of *TaSUT* genes was diverse, and the number of exons was the smallest in *TaSUT5A*, which had four exons, and the largest in *TaSUT1A*, which had 11 exons. The lengths of the genes were mostly between 3 and 6 kb, whereas *TaSUT3A* and *TaSUT3D* had distinctively long gene lengths of 34 kb and 47 kb, respectively (Fig. 2A).

Phylogenetic tree analysis was performed to investigate the evolutionary relationships among the *SUT* gene families in different plant species, such as maize, rice, barley, *Brachypodium*, and *Arabidopsis* (Fig. 3). *TaSUT* genes are closely related to various *SUT* families in other species. Based on the phylogenetic relationships in previous research (Braun and Slewinski, 2009; Kühn and Grof, 2010; Lalonde and Frommer, 2012; Wang et al., 2021), SUT proteins, including the newly identified TaSUT proteins, were classified into five groups. TaSUT1 and TaSUT3 appeared in the SUT3 group, which was a monocot-specific group, whereas TaSUT2 appeared in the SUT4 group, a group shared by both monocots and dicots. TaSUT4, was also classified in a common group of monocots and dicots and appeared in the SUT2 group. TaSUT5, TaSUT6, and TaSUT7 was categorized under the SUT5 group which is another monocot specific group.

3.2. Chromosomal localization and synteny analysis of TaSUT genes

TaSUT gene localization was predicted using the IWGSC RefSeq v2.1 (Fig. 4). Most of the genes had homoeologs in all the subgenomes; however, the A genome homoeolog of *TaSUT2* and the B genome homoeologs of *TaSUT3* and *TaSUT7* were not present. The *TaSUT* genes were present in diverse chromosomes: *TaSUT1* in Chr. 4, *TaSUT2* in Chr.5, *TaSUT3* in Chr. 1, *TaSUT4* in Chr. 6, *TaSUT5* in Chr. 4 and 5, *TaSUT6* in Chr. 2, and *TaSUT7* in Chr. 7. While most of the genes were located in a similar position in each subgenome, *TaSUT1A* and *TaSUT5A* were differentially localized from their homoeologs.

Synteny analysis revealed that synteny in the genome was highly

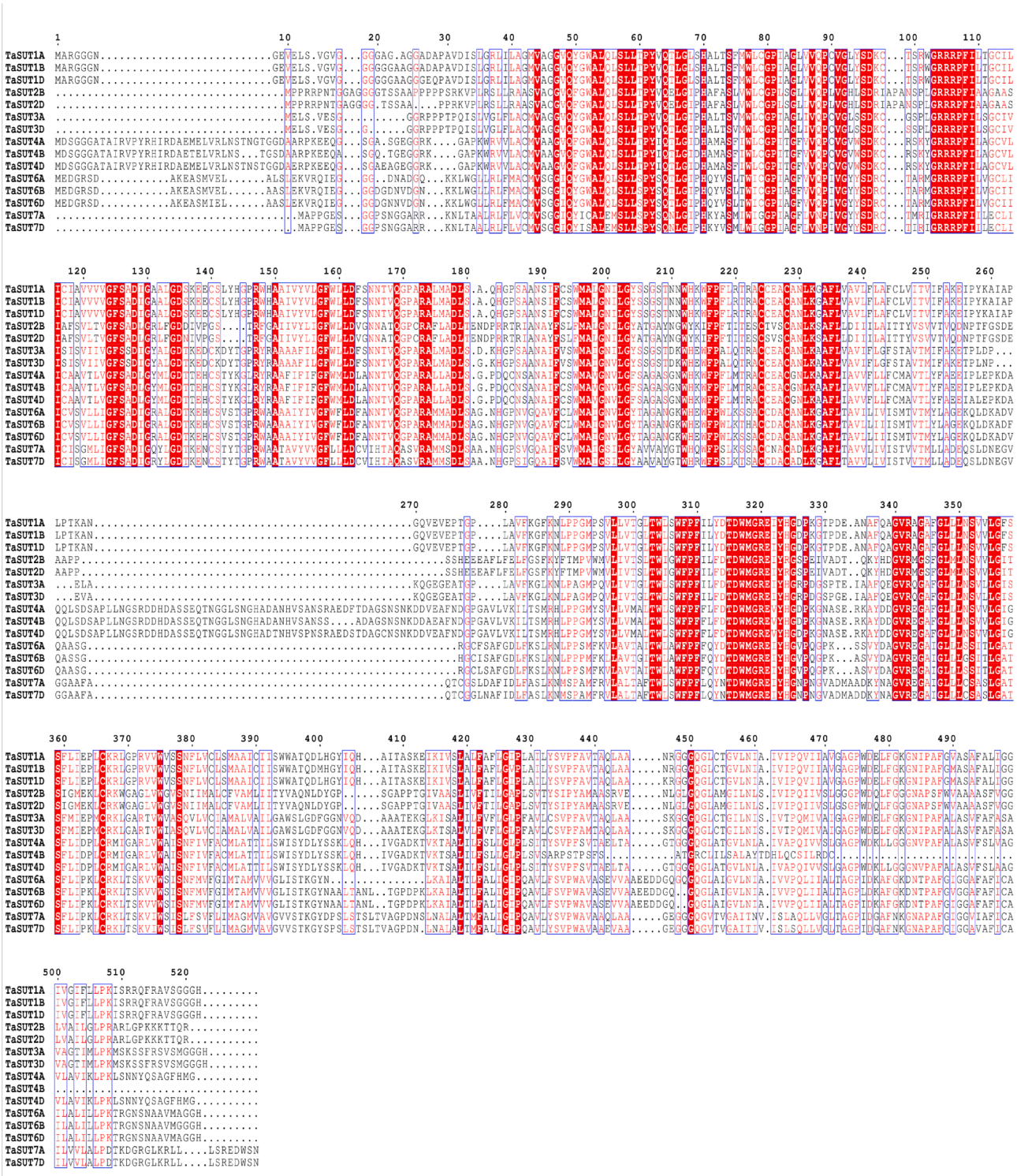

Fig. 1. Amino acid sequence alignment of all TaSUT proteins. Amino acid sequences were aligned using the Clustal W tool. The similarity in the amino acids across all sequences is highlighted. The identical sequences and the highly similar sequences are represented with red boxes and red text color, respectively. (For interpretation of the references to color in this figure legend, the reader is referred to the web version of this article.)

conserved between wheat and rye, barley, and *Brachypodium* (Fig. 5). The synteny of *TaSUT* genes was differentially observed between each pair of species. The synteny of *TaSUT1* and *TaSUT2* was observed in all the species. In contrast, synteny was represented for *TaSUT4* in barley and *Brachypodium*, *TaSUT6* in rye and barley, *TaSUT3* in barley, and *TaSUT5* in rye.

3.3. *Cis-acting regulatory elements in the TaSUT gene promoters*

To elucidate the potential roles of *cis*-acting regulatory elements in *TaSUT* genes, 1.5 kb upstream of each *TaSUT* gene sequence was analyzed (Table S1). Most of the identified *cis*-elements were classified into five groups depending on their functions. A total of 1,467 *cis*-

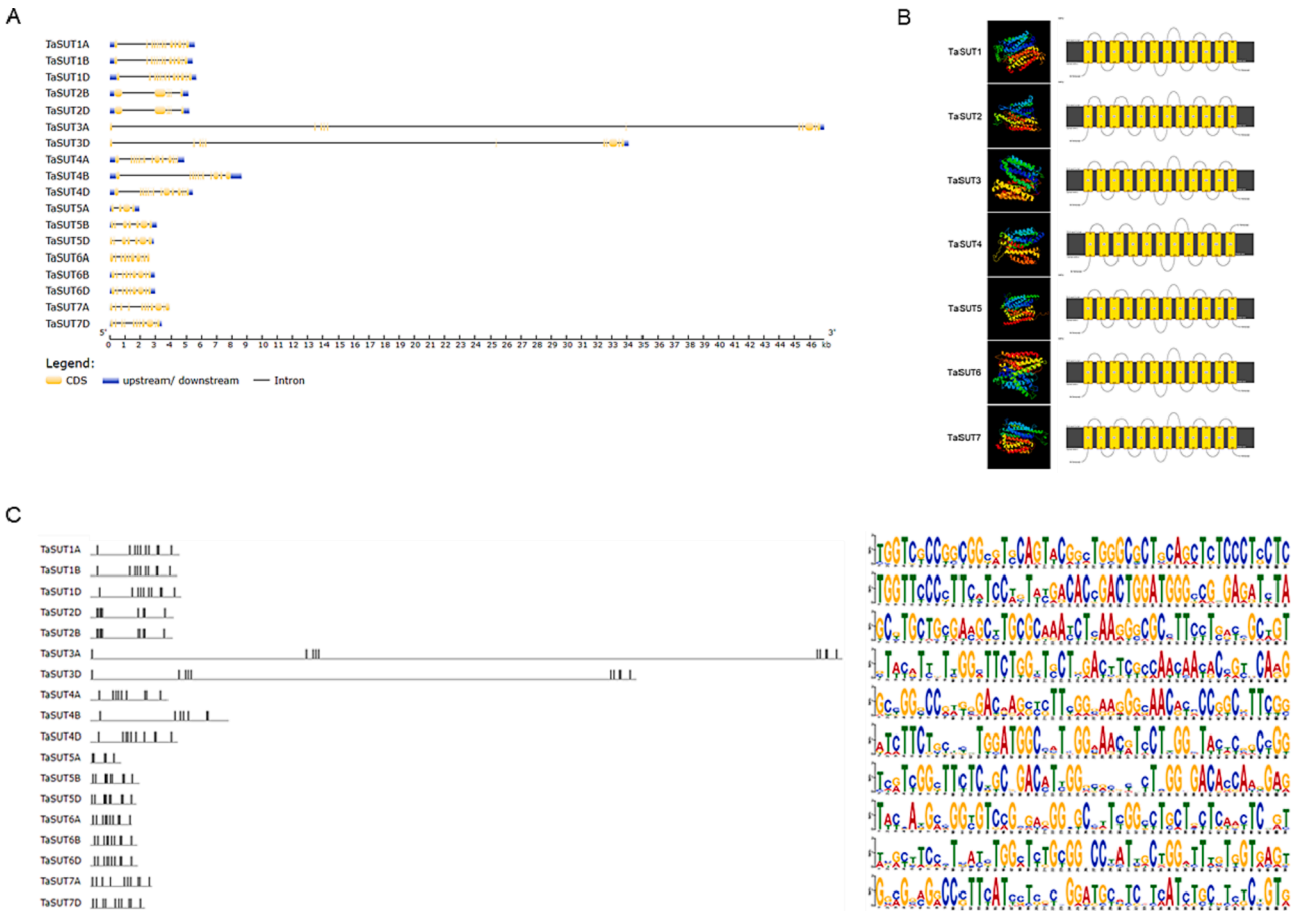

Fig. 2. (A) The exon-intron structure of *TaSUT* genes. The yellow and blue boxes and the black lines indicate coding sequences (CDS), UTRs and introns, respectively. (B) Predicted 3D structure of TaSUT proteins and transmembrane regions are presented. (C) Conserved motifs in *TaSUT*s. The left and the right figure represents the position of the motifs, and the conserved sequences of each motif, respectively. (For interpretation of the references to color in this figure legend, the reader is referred to the web version of this article.)

elements were identified, among which 192 were light-responsive, 66 were stress-related, 153 were phytohormone-related, 129 were MYB-related, and 82 were MYC-related regulatory elements. Notably, all sequences had at least one of the elements from each category except for *TaSUT2U* and *TaSUT7A*, which did not have any MYC-related elements. The highest number of *cis*-elements was the CAAT-box (331) regulatory element that functions in the promoter and enhancer regions, followed by the TATA-box (207), which specifies the transcription start site. In addition, 845 *cis*-elements with diverse known and unknown functions have been identified. *Cis*-elements with known functions include RY-elements (CATGCA sequence) which are involved in seed-specific regulation; O2-site, which functions in zein metabolism regulation; MSA-like (mitosis-specific activator-like) element regulating cell cycle; CAT-box functioning in meristem expression; and Box III element, which is involved in protein binding sites.

To elucidate the correlation between the existence of specific types of *cis*-elements and actual gene expression, we observed the gene expressions during diurnal cycle and in response to ABA or MeJA treatment. (Fig. S2). It was shown that *SUT*s have different expression patterns during diurnal cycle, but all of them change in response to light (Fig. S2A). In addition, all of the *SUT*s except for *SUT1* were up-regulated in response to ABA (Fig. S2B) or MeJA (Fig. S2C) treatment, which implies *SUT*s might be regulated by factors binding to their *cis*-elements in the promoters.

3.4. Subcellular localization and protoplast esculin assay of TaSUT proteins

The coding sequences of *TaSUT1*, *TaSUT2*, *TaSUT3*, *TaSUT4*, *TaSUT6*, and *TaSUT7* were fused with GFP to produce GFP fusion protein constructs. *TaSUT5* was identified to have an insertion mutation and was not expressed (Fig. S1). All GFP-TaSUT fusion proteins were identified as plasma membrane proteins (Fig. 6). TaSUT2 was also expressed in the tonoplast.

The GFP-fused constructs were also utilized for the esculin uptake assay to identify whether each *TaSUT* gene was an active sucrose transporter using the fluorescent sucrose analog esculin. Confocal analysis of GFP and esculin fluorescence revealed that protoplasts labeled with GFP-TaSUT1, GFP-TaSUT2, and GFP-TaSUT6 actively took up esculin. However, GFP-TaSUT4 exhibited minimal uptake of the esculin analog in its vacuole, and that esculin uptake was limited to the plasma membrane. GFP-TaSUT3 and GFP-TaSUT7 also demonstrated relatively less esculin uptake within cells.

3.5. In silico wheat tissue-specific expression

Tissue-specific gene analysis revealed that *TaSUT1* and *TaSUT2* were highly expressed in the stem tissues at Z32 and Z65 (Fig. 7). *TaSUT1* was also highly expressed in the leaves at Z23 and Z71, whereas *TaSUT2* was also highly expressed in grains at Z85 and the roots. *TaSUT3* was highly expressed in the spike at Z65, whereas *TaSUT4* was mainly expressed in the roots at all stages. *TaSUT5* was highly expressed in the spike at Z65,

Fig. 3. Phylogenetic analysis of selected plant sucrose transporters and their homologs. Phylogenetic tree of SUT proteins constructed using the neighbor-joining tree method with MEGA X software program. TaSUT: *Triticum aestivum* (wheat), HORVU: *Hordeum vulgare* (barley), BRADI: *Brachypodium distachyon*, OsSUT: *Oryza sativa* (rice), ZmSUT: *Zea mays* (maize), AtSUT: *Arabidopsis thaliana.*

as well as in the grain at Z71. *TaSUT6*, along with *TaSUT7*, were also highly expressed in grains at Z71.

3.6. Gene expression under abiotic stress treatment

"Keumgang" seedlings were exposed to cold, heat, salt, drought, and osmotic stress treatments to determine the variation in the expression levels of the *TaSUT* genes at four-time intervals: 0 h (control), 6 h, 12 h, and 24 h (Fig. 8&S3). Notably, *TaSUT2* expression was majorly upregulated at 12 and 24 h under cold stress. *TaSUT1* expression levels significantly decreased after 6 h of treatment, followed by a spike in the expression at 12 h. *TaSUT3* and *TaSUT7* expression levels significantly increased after 24 h of treatment, whereas *TaSUT6* exhibited a consistent decline in expression levels.

Under heat stress, *TaSUT1* and *TaSUT2* expression levels declined significantly, whereas *TASUT3* exhibited maximum expression levels at all time intervals. *TaSUT4* expression levels also increased significantly at 6 and 12 h; however, the expression levels significantly decreased at 24 h. *TaSUT6* expression increased at 12 and 24 h, whereas *TaSUT7* expression increased significantly at 24 h.

Under salt stress, *TaSUT1*, *TaSUT3*, and *TaSUT7* expression levels gradually declined, whereas *TaSUT2* expression levels recovered at 24 h. *TaSUT4* levels significantly declined at 6 and 12 h; however, at 24 h, *TaSUT4* levels were considerably increased. *TaSUT6* displayed the highest expression under salt stress and increased almost five-fold at 24 h.

Under drought stress, *TaSUT1*, *TaSUT3*, and *TaSUT6* expression levels were significantly downregulated, whereas those of *TaSUT4* and *TaSUT7* declined at 6 h; however, at 12 and 24 h, there was no significant difference in their expression. *TaSUT2* expression increased at 6 and 12 h, followed by an insignificant difference at 24 h.

Lastly, sucrose-induced osmotic stress demonstrated minimal effects on *TaSUT* genes. *TaSUT1*, *TaSUT2*, and *TaSUT6* were unaffected by treatment. *TaSUT4* expression declined at 6 h, which was followed by an insignificant difference. In contrast to *TaSUT4*, *TaSUT7* expression significantly declined at 24 h and was insignificantly different at earlier time intervals. *TaSUT3* was the only gene substantially affected by sucrose treatment, and their expression levels were elevated fourfold compared to the expression level in the control.

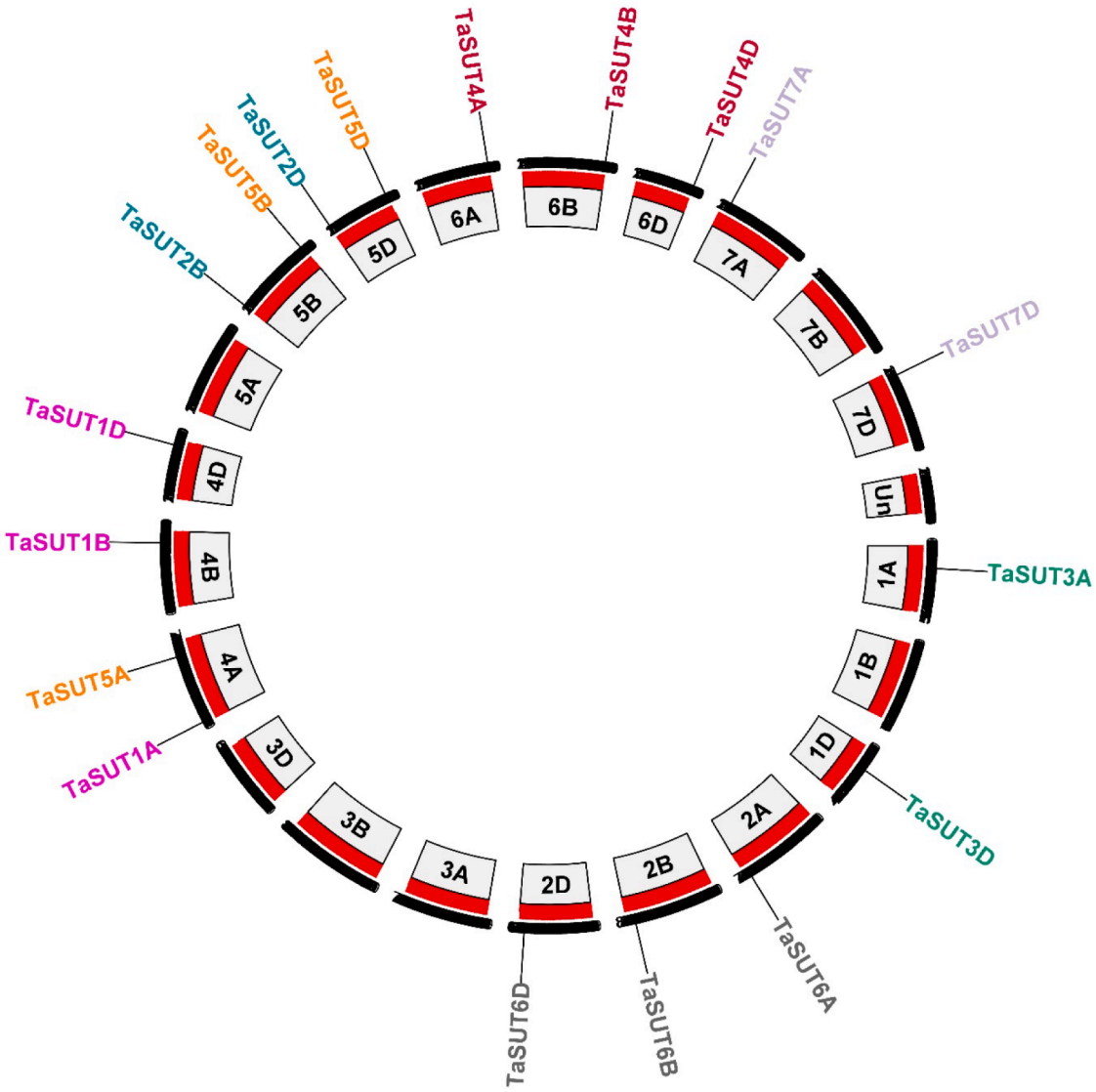

Fig. 4. Chromosomal localization of the *TaSUT* genes. The image was created using the MapChart application software. Three *TaSUT* genes were located on each chromosome except chromosome 5D, where four *TaSUT* genes were localized.

4. Discussion

Sucrose transporter genes belong to the MFS family and play a vital role in the sucrose transport system of plants. The sucrose transporters carry the glucose synthesized in the photosynthetic tissues to all the cells, which require energy for their metabolic functions. Plants convert glucose into sucrose for its effective transport owing to its increased stability, water solubility, and energy efficiency compared to glucose (Aluko et al., 2021). To the best of our knowledge, wheat has two sucrose transporter genes, *TaSUT1* and *TaSUT2* (Aoki et al., 2002; Deol et al., 2013). In this study, we identified five new *SUT*s in wheat, suggesting that at least seven *SUT*s are present in wheat (Fig. 1). The newly identified genes are clearly distinguishable with the previously identified *SUT1* and *SUT2* especially in the gene expression patterns. *SUT3*, *SUT6*, *SUT7* are mostly expressed in wheat spike or grain (Fig. 7), and also each gene has diverse responses to different types of abiotic stress (Fig. 8). The number of *SUT*s in the wheat genome is similar to the number in the other species. The maize genome also contains seven *SUT*s (Leach et al., 2017), whereas rice and *Arabidopsis thaliana* contain five (Aoki et al., 2003; Iqbal et al., 2020) and nine genes, respectively (Pommerrenig et al., 2013; Rottmann et al., 2018). SUT proteins typically have 12 transmembrane domains to efficiently transport sugar through the cell membrane (Lalonde et al., 2004). The 3D structure prediction represented that most TaSUT proteins contain 12 transmembrane domains, except for TaSUT4, highlighting their functions as sugar transporters (Fig. 2B).

The exon-intron structure analysis revealed that *TaSUT3A* and *TaSUT3D* have extremely large introns, which make the entire length of 47 kb and 34 kb for each gene. The homologs of these genes in barley (HORVU.MOREX.r3.1HG0037550) and rye (ScWN1R01G186600) also have similar gene structures and have gene length of 69,324 bp and 41,833 bp, respectively. It is thought that *TaSUT3* homologs are thought to have been recently diverged from their common ancestors, because they are not even found in the genome of closely related model plant *Brachypodium*. *TaSUT3*s have distinct tissue-specific gene expression compared to the other genes in that they are specifically expressed in spike at Z65 (Fig. 7) and are also highly responsive to sucrose treatment (Fig. 8). However, whether the structures of these genes affect their own gene expressions remains to be elucidated in future studies.

Phylogenetic tree analysis revealed that the *SUT* gene family in

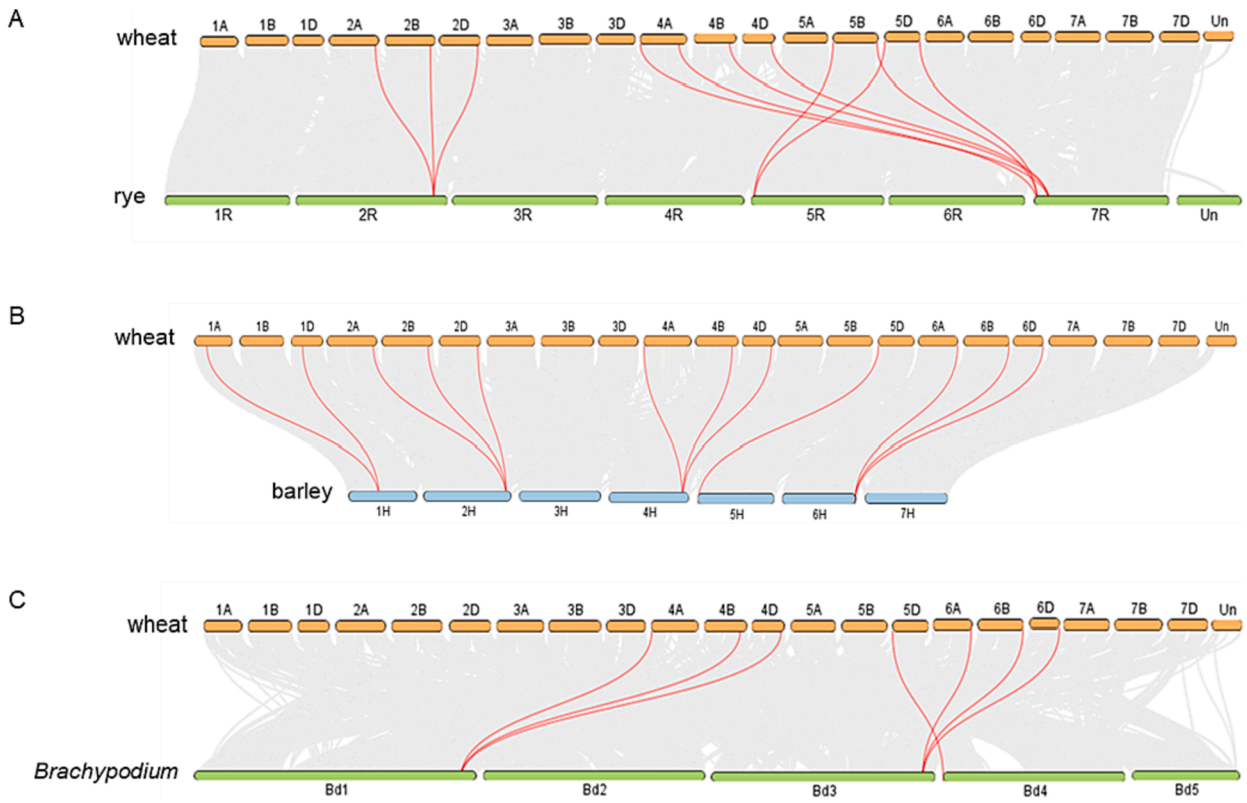

Fig. 5. Synteny analysis of *Triticum aestivum* genome with its closely related species, (A) rye, (B) barley, and (C) *Brachypodium*. The gray lines represent aligned blocks between the paired genomes, and the red lines indicate syntenic *SUT* gene pairs. Visualization was performed using Dual Synteny Plot in TBtools (v1.09876). (For interpretation of the references to color in this figure legend, the reader is referred to the web version of this article.)

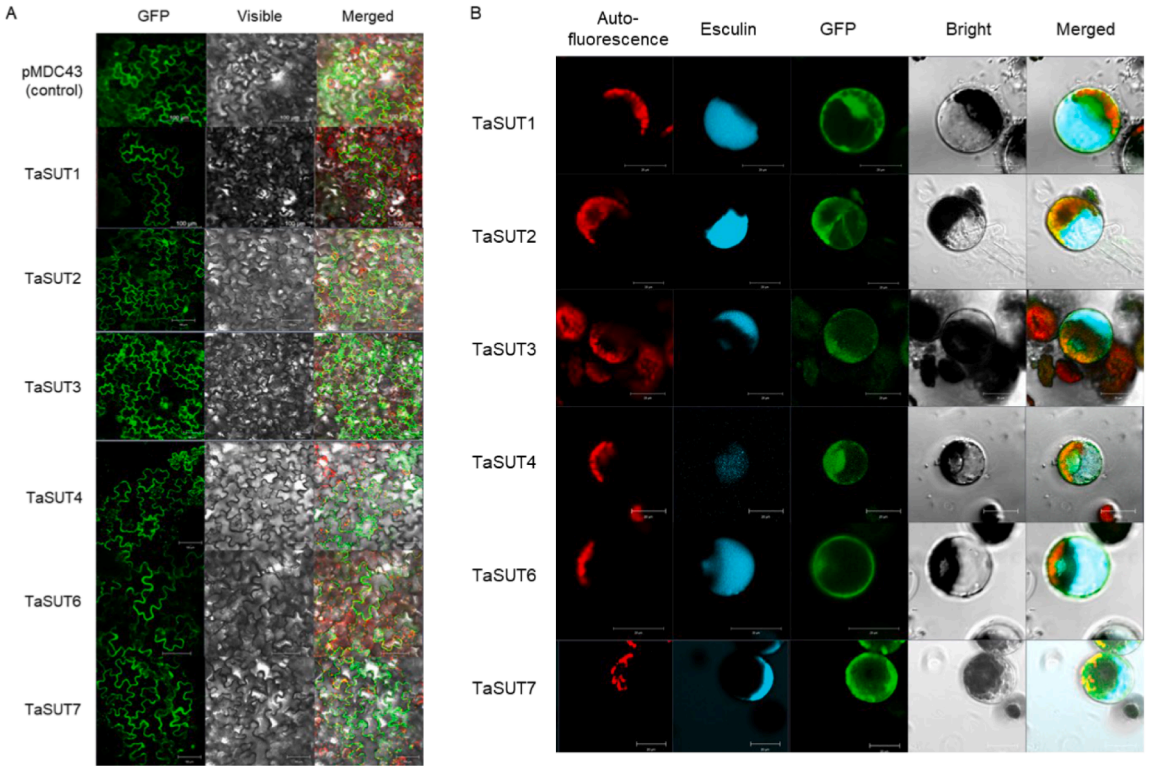

Fig. 6. (A) Subcellular localization of GFP tagged TaSUT proteins in tobacco (*Nicotina tabacum*) leaves. (B) Uptake of the fluorescent sucrose analog, esculin, by the sucrose transporter genes as imaged by confocal microscopy.

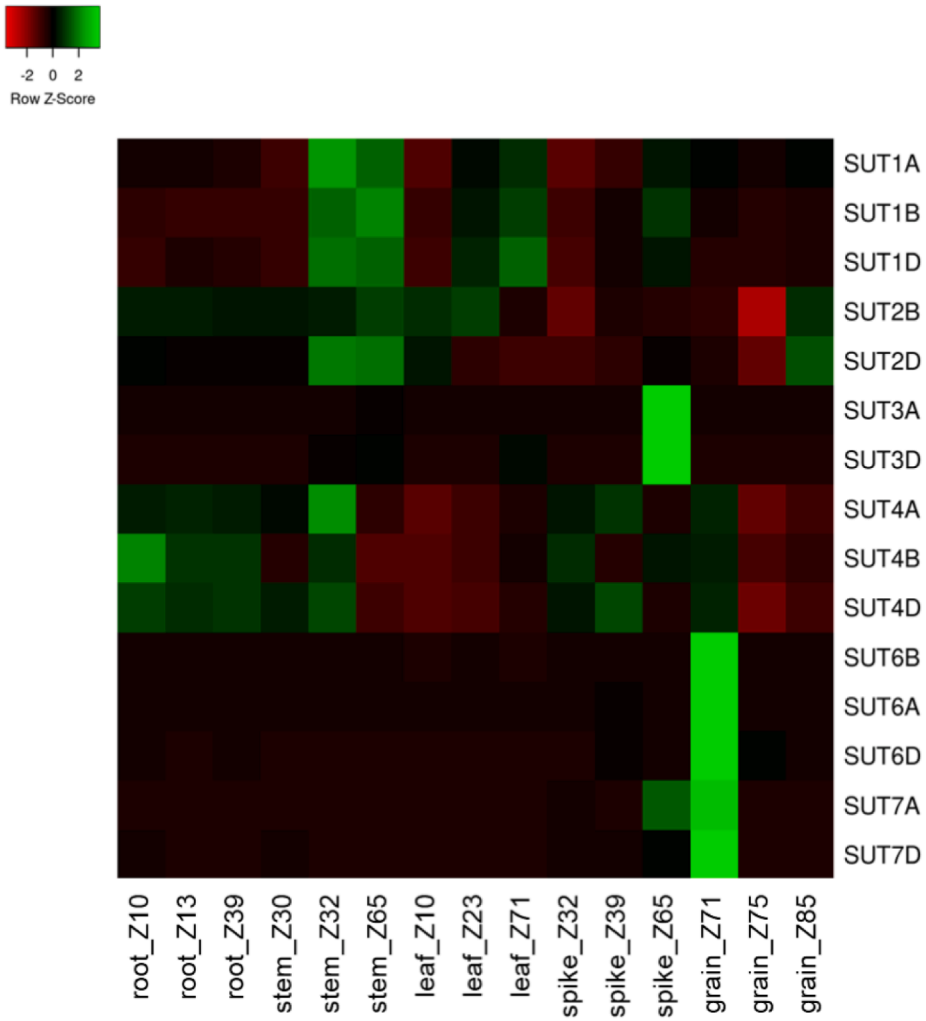

Fig. 7. Heat map of wheat tissue-specific gene expression of *TaSUT* genes. The genes were clustered using the average linkage method with Euclidean distance measurement. Z; Zadoks scale.

plants diverged and can eventually be classified into five groups (Fig. 3). Particularly, each monocot (*SUT3* and *SUT5*) and dicot specific groups (*SUT1*) were present, implying that a large evolutionary change occurred between monocots and dicots. The differences in the number of *SUT* gene families in each monocot (seven in maize and five in rice) and dicot (nine in *Arabidopsis* and 11 in tobacco) (Wang et al., 2019) also indicate that these two types of plants are evolutionarily distant.

Chromosomal localization of *TaSUT* genes revealed that the homoeologs of each gene were located similar positions in each sub-genome (Fig. 4). *SUT3B* and *SUT7B*, which may have been degenerated during evolution, were not identified. *SUT2A*, which had been published in a previous study (Deol et al., 2013), was also not identified in our study. Since the previous study used wheat cultivar 'AC Andrew' to clone the gene, it is thought that the presence of *SUT2A* depends on the types of cultivar, and it is absent in 'Chinese Spring'. Furthermore, *SUT1A* and *SUT5A* in Chr.4A were present at distinct positions compared to their homoeologs. Chr.4A had inverted synteny with Chr.4B (Ling et al., 2018) and the distal regions of Chr.5B and Chr.5D had different synteny with Chr.5A (Li et al., 2021). Therefore, *SUT1A* and *SUT5A* located in these regions might have distinct positions from their homoeologs. This phenomenon was also observed in synteny analysis (Fig. 5). Furthermore, the number of syntenic genes between the two species was smaller in wheat-*Brachypodium* than in wheat-rye and wheat-barley. This is consistent with a previous report that wheat has a greater genetic distance from *Brachypodium* than from rye or barley (Escobar et al., 2011).

The *cis*-element analysis results suggested that the promoters of *TaSUT* genes consisted of various *cis*-elements, which could be divided into five main categories: light responsive, stress-related elements, phytohormone-related elements, MYB elements, and MYC-related elements (Table S1). Light and photoperiodism are associated with photosynthesis in plants. The more the light and sufficient amount of carbon and water, the more photosynthesis occurs, and thus the higher the production and distribution of photosynthates. Hence, the number of light-responsive elements is expected to be higher in *SUT* promoters. Light intensity is essential for the upregulation of SUT proteins and its role in phloem loading and unloading (Baker et al., 2016; Chincinska et al., 2013; Xu et al., 2020). In this study, many phytohormone-stress-related elements were identified. Phytohormone elements such as ABRE-, TGACG-, and CGTCA-motifs (both methyl jasmonate-responsive) were present in greater numbers, along with TGA (auxin (IAA) responsive), TCA (salicylic responsive), and P-box (gibberellin (GA)-responsive) elements. ABRE is an abscisic acid response element. Research conducted on sweet potato (*Ipomoea batatas* (L.) Lam) revealed that *IbSUT4* is involved in plant growth and is an important positive regulator of plant stress tolerance through the ABF-dependent ABA signaling pathway (Wang et al., 2020). Li et al. investigated the role of *SUT* genes in response to plant hormones using qRT-PCR in tetraploid cotton

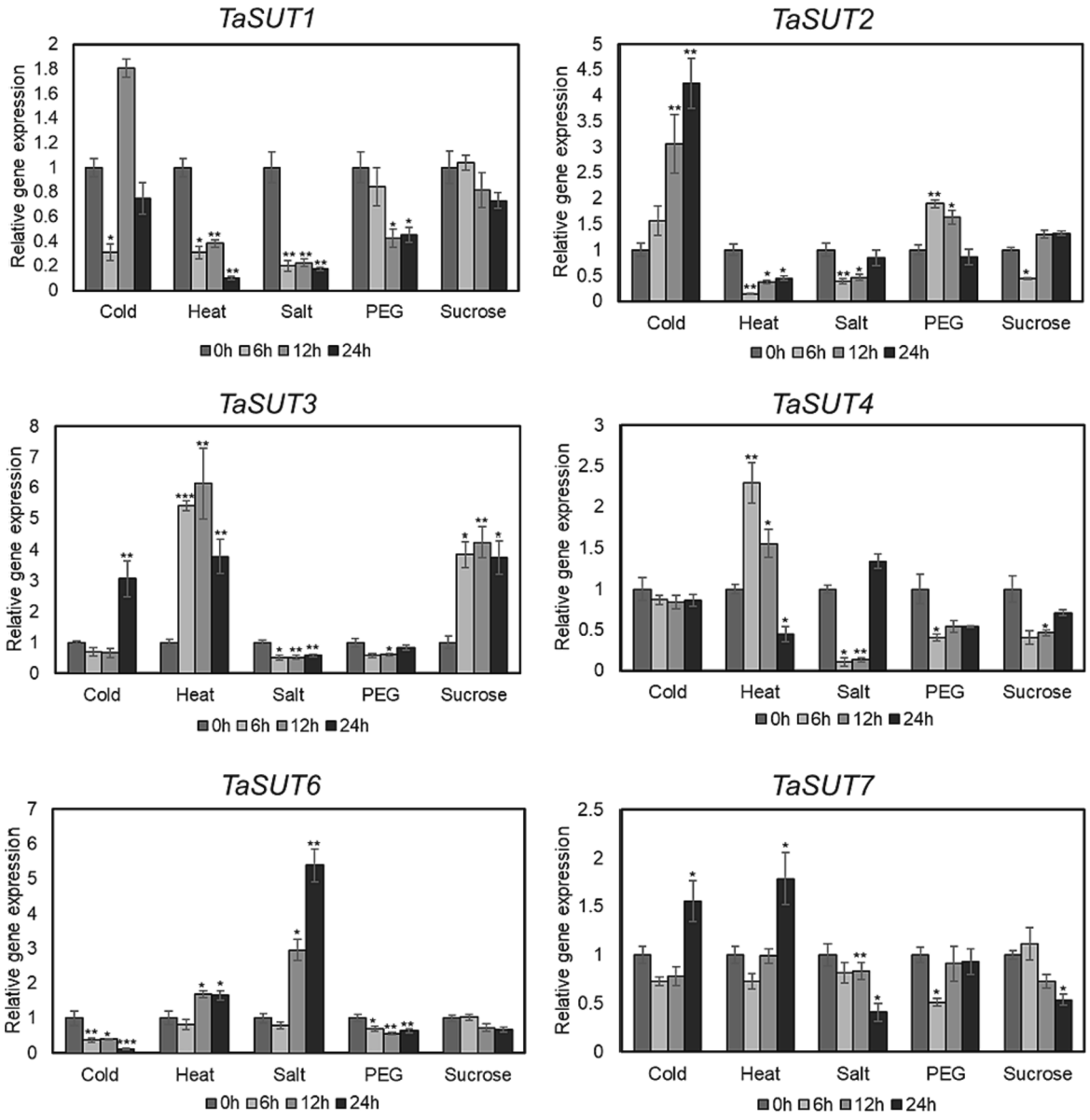

Fig. 8. *TaSUT* gene expression in response to abiotic treatments. The error bars indicate the standard error of the means (n = 3). Significant differences of the expression levels between each time point and 0 h are indicated by the asterisks between the control (no treatment) and the stress-treated plants (*p < 0.05, **p < 0.01, ***p < 0.001).

Gossypium hirsutum (Li et al., 2018). Their results indicated that *GhSUT*s were significantly upregulated until 3 h of IAA treatment, and GA treatment also demonstrated significant differences in expression by displaying upregulation for the first hour, followed by downregulation. Salicylic acid treatment also exhibited diverse expression patterns among *GhSUT* genes. Thus, the *cis*-acting regulatory elements in promoter regions and expression profiling under different abiotic stress and exogenous phytohormone conditions implied that *SUT* genes might play an indispensable role in plant responses to diverse abiotic stresses and phytohormones.

GFP analysis of *TaSUT*s confirmed the plasma membrane expression of all proteins in this family except TaSUT2, which was expressed in the tonoplast, consistent with a previous report (Deol et al., 2013) (Fig. 6A). Among the identified genes, *TaSUT5* was found to be mutated with additional nucleotides in the gene coding sequence (Fig. S1). This was also in agreement with the *in-silico* data, which revealed that *TaSUT5*, was expressed at negligible levels. This may indicate the non-functionality of *TaSUT5*, which may exist as a pseudogene. Moreover, the individual functionality of TaSUTs was assessed using the protoplast esculin uptake assay (Fig. 6B). For a sucrose transporter to be considered an active transporter, esculin should actively exhibit bright fluorescence inside the cell vacuole. All SUTs had taken esculin into their cell vacuoles. The clearest and most prominent uptake of esculin was by TaSUT1, TaSUT2, and TaSUT6, demonstrating greater esculin uptake than the other transporters. The weakest fluorescence was observed for TaSUT4. TaSUT3 and TaSUT7 also exhibited weaker fluorescence than the other TaSUT proteins. A plausible reason for the limited esculin uptake by these may be attributed to their involvement in low energy-requiring processes. Therefore, bulk transportation may not be required or the two transporters other substrates or participate in other regulatory functions unrelated to transport activity. (Rottmann et al., 2018).

Wheat tissue-specific gene expression analysis revealed that TaSUTs are expressed in various parts of the plant, including the roots, stems, leaves, spikes, and grains. The heatmap results demonstrated higher *TaSUT1* expression in the stems, leaves, and spike tissues of wheat. Research on maize (*Zea mays*) revealed that *ZmSUT1* mutants had

significantly reduced stature, altered biomass partitioning, delayed flowering, and stunted tassel development (Slewinski et al., 2009) correlating with the heatmap expression data obtained for wheat. Similarly, under field conditions, *ZmSUT2* mutant plants grew slower, possessed smaller tassels and ears, and produced fewer kernels than wild-type siblings (Leach et al., 2017). The *TaSUT2* data revealed higher expression in stems, leaves, and grains. Overexpression of pear *PbSUT2* (*Pyrus bretschneideri*) in tomato (*Solanum lycopersicum*) led to an increase in the net photosynthetic rate in leaves and sucrose content in mature fruit compared to that in wild-type tomato plants. This indicates that *PbSUT2* affects the sucrose content in sinks and the flowering phase, thereby promoting plant growth and development (Wang et al., 2016). *TaSUT3*, *TaSUT4*, *TaSUT5*, *TaSUT6*, and *TaSUT7* were mainly expressed in spike and grain tissues. PttSUT3 (*Populus tremula* × *Populus tremuloides*) has been identified as a principal transporter for carbon delivery into secondary cell wall-forming wood fibers (Mahboubi et al., 2013), whereas *StSUT4* in potato (*Solanum tuberosum*) has been demonstrated to affect flowering (Chincinska et al., 2013). Expression of *TaSUT5*, *TaSUT6*, and *TaSUT7*, particularly in the spike and grain, indicates more limited functionality within the confines of the tissue; however, further research is required to fully explore the diverse and differential expression of all sucrose transporters in wheat.

In addition, gene expression of *TaSUT*s to abiotic factors, cold, heat, salt, drought, and osmotic stress, was identified. Previous studies have indicated that *SUT*s play a role in stress signaling by regulating sugar status (Kaur et al., 2021; Wang et al., 2020; Xu et al., 2018). Research on *Arabidopsis thaliana* (Gong et al., 2015) demonstrated that the loss of function of *AtSUC2* and *AtSUC4*, resulted in seedlings being overly sensitive to drought, cold, and salt stress. This indicated the prominent role of SUCs/SUTs in stress response. This was also clearly seen in the *TaSUT2* expression levels under various stress treatments, especially the cold treatment, as well as in the PEG-6000-induced drought stress. *TaSUT3* also seems to play a critical role in heat and sucrose-induced osmotic stress, as the expression levels were much higher than those in the controls. *TaSUT4* and *TaSUT6* likely engage in heat and salt stress, respectively (Fig. 8). Based on our results of *TaSUT* gene expression, we hypothesize that *TaSUT* genes may play a vital role in stabilizing plants under stress by actively regulating cellular sugar levels. The effect of various stresses is observable through changes in the expression levels of *TaSUT*s; however, the effect of stress on sucrose distribution and the fundamental mechanism of this effect are yet to be explored (Wang et al., 2020).

In summary, five novel sucrose transporter genes were identified in wheat in this study, resulting in a total of seven SUTs in the wheat genome. *TaSUT*s have been categorized into five available sucrose transporter clades according to their phylogeny. Moreover, we identified the remaining *SUT* genes in wheat and verified their localization and functionality in terms of transportation. We believe that our study would serve as a foundation to better understand the large and highly complex hexaploid wheat genome.

5. Funding

This work was conducted with the support of the "Basic Science Research Program" through the National Research Foundation of Korea (NRF), funded by the Ministry of Education (2021R1I1A1A01048945), and a grant from the Korea University, Republic of Korea.

6. Consent for publication

All authors agreed to submit this paper for publication.

7. Availability of data and material.

All data generated or analyzed during this study are included in this published article and its supplementary information files.

CRediT authorship contribution statement

Depika Prasad: Conceptualization, Data curation, Formal analysis, Writing - original draft. **Woo Joo Jung:** Conceptualization, Data curation, Formal analysis, Writing - original draft. **Yong Weon Seo:** Investigation, Supervision, Writing - review & editing.

Declaration of Competing Interest

The authors declare that they have no known competing financial interests or personal relationships that could have appeared to influence the work reported in this paper.

Data availability

No data was used for the research described in the article.

Appendix A. Supplementary data

Supplementary data to this article can be found online at https://doi.org/10.1016/j.gene.2023.147245.

References

Aluko, O.O., Li, C., Wang, Q., Liu, H., 2021. Sucrose utilization for improved crop yields: A review article. Int. J. Mol. Sci. 22, 4704.
Aoki, N., Hirose, T., Scofield, G.N., Whitfeld, P.R., Furbank, R.T., 2003. The sucrose transporter gene family in rice. Plant Cell Physiol. 44, 223–232.
Aoki, N., Whitfeld, P., Hoeren, F., Scofield, G., Newell, K., Patrick, J., Offler, C., Clarke, B., Rahman, S., Furbank, R.T., 2002. Three sucrose transporter genes are expressed in the developing grain of hexaploid wheat. Plant Mol. Biol. 50, 453–462.
Babicki, S., Arndt, D., Marcu, A., Liang, Y., Grant, J.R., Maciejewski, A., Wishart, D.S., 2016. Heatmapper: Web-enabled heat mapping for all. Nucleic Acids Res. 44, W147–W153.
Baker, R.F., Leach, K.A., Boyer, N.R., Swyers, M.J., Benitez-Alfonso, Y., Skopelitis, T., Luo, A., Sylvester, A., Jackson, D., Braun, D.M., 2016. Sucrose transporter *ZmSUT1* expression and localization uncover new insights into sucrose phloem loading. Plant Physiol. 172, 1876–1898.
Braun, D.M., Slewinski, T.L., 2009. Genetic control of carbon partitioning in grasses: Roles of sucrose transporters and tie-dyed loci in phloem loading. Plant Physiol. 149, 71–81.
Burkle, L., Hibberd, J.M., Quick, W.P., Kuhn, C., Hirner, B., Frommer, W.B., 1998. The H +-sucrose cotransporter *NtSUT1* is essential for sugar export from tobacco leaves. Plant Physiol. 118, 59–68.
Cai, Y., Tu, W., Zu, Y., Jing, Y., Xu, Z., Lu, J., Zhang, Y., 2017. Overexpression of a grapevine sucrose transporter (*VvSUC27*) in tobacco improves plant growth rate in the presence of sucrose in vitro. Front. Plant Sci. 8, 1069.
Chandran, D., Reinders, A., Ward, J.M., 2003. Substrate specificity of the *Arabidopsis thaliana* sucrose transporter *AtSUC2*. J. Biol. Chem. 278, 44320–44325.
Chen, C., Chen, H., Zhang, Y., Thomas, H.R., Frank, M.H., He, Y., Xia, R., 2020. TBtools: An integrative toolkit developed for interactive analyses of big Biological Data. Mol. Plant. 13, 1194–1202.
Chen, H., Nelson, R.S., Sherwood, J.L., 1994. Enhanced recovery of transformants of *Agrobacterium tumefaciens* after freeze-thaw transformation and drug selection. BioTechniques. 16, 664.
Cheng, J., Wen, S., Xiao, S., Lu, B., Ma, M., Bie, Z., 2018. Overexpression of the tonoplast sugar transporter *CmTST2* in melon fruit increases sugar accumulation. J. Exp. Bot. 69, 511–523.
Chincinska, I., Gier, K., Krügel, U., Liesche, J., He, H., Grimm, B., Harren, F.J., Cristescu, S.M., Kühn, C., 2013. Photoperiodic regulation of the sucrose transporter *StSUT4* affects the expression of circadian-regulated genes and ethylene production. Front. Plant Sci. 4, 26.
Dasgupta, K., Khadilkar, A.S., Sulpice, R., Pant, B., Scheible, W.R., Fisahn, J., Stitt, M., Ayre, B.G., 2014. Expression of sucrose transporter cDNAs specifically in companion cells enhances phloem loading and long-distance transport of sucrose but leads to an inhibition of growth and the perception of a phosphate limitation. Plant Physiol. 165, 715–731.
Deol, K.K., Mukherjee, S., Gao, F., Brûlé-Babel, A., Stasolla, C., Ayele, B.T., 2013. Identification and characterization of the three homeologues of a new sucrose transporter in hexaploid wheat (*Triticum aestivum* L.). BMC Plant Biol. 13, 181–181.
Escobar, J.S., Scornavacca, C., Cenci, A., Guilhaumon, C., Santoni, S., Douzery, E.J.P., Ranwez, V., Glémin, S., David, J., 2011. Multigenic phylogeny and analysis of tree incongruences in Triticeae (Poaceae). BMC Evol. Biol. 11, 181.
Finegan, C., Boehlein, S.K., Leach, K.A., Madrid, G., Hannah, L.C., Koch, K.E., Tracy, W. F., Resende, M.F.R., Jr.,, 2021. Genetic perturbation of the starch biosynthesis in maize endosperm reveals sugar-responsive gene networks. Front. Plant Sci. 12, 800326.

Frost, C.J., Nyamdari, B., Tsai, C.J., Harding, S.A., 2012. The tonoplast-localized sucrose transporter in Populus *(PtaSUT4)* regulates whole-plant water relations, responses to water stress, and photosynthesis. PLoS One. 7, e44467.
Gong, X., Liu, M., Zhang, L., Ruan, Y., Ding, R., Ji, Y., Zhang, N., Zhang, S., Farmer, J., Wang, C., 2015. Arabidopsis *AtSUC2* and *AtSUC4*, encoding sucrose transporters, are required for abiotic stress tolerance in an ABA-dependent pathway. Physiol. Plant. 153, 119–136.
Gottwald, J.R., Krysan, P.J., Young, J.C., Evert, R.F., Sussman, M.R., 2000. Genetic evidence for the in-planta role of phloem-specific plasma membrane sucrose transporters. Proc. Natl Acad. Sci. U. S. A. 97, 13979–13984.
Hu, B., Jin, J., Guo, A.Y., Zhang, H., Luo, J., Gao, G., 2015. GSDS 2.0: An upgraded gene-feature visualization server. Bioinformatics. 31, 1296–1297.
Iqbal, S., Ni, X., Bilal, M.S., Shi, T., Khalil-Ur-Rehman, M., Zhenpeng, P., Jie, G., Usman, M., Gao, Z., 2020. Identification and expression profiling of sugar transporter genes during sugar accumulation at different stages of fruit development in apricot. Gene. 742, 144584.
Jiang, S.Y., Chi, Y.H., Wang, J.Z., Zhou, J.X., Cheng, Y.S., Zhang, B.L., Ma, A., Vanitha, J., Ramachandran, S., 2015. Sucrose metabolism gene families and their biological functions. Sci. Rep. 5, 17583.
Kariya, K., Sameeullah, M., Sasaki, T., Yamamoto, Y., 2017. Overexpression of the sucrose transporter gene *NtSUT1* alleviates aluminum-induced inhibition of root elongation in tobacco (*Nicotiana tabacum* L.). Soil Sci. Plant Nutr. 63, 45–54.
Kaur, H., Manna, M., Thakur, T., Gautam, V., Salvi, P., 2021. Imperative role of sugar signaling and transport during drought stress responses in plants. Physiol. Plant. 171, 833–848.
Kelley, L.A., Mezulis, S., Yates, C.M., Wass, M.N., Sternberg, M.J.E., 2015. The Phyre2 web portal for protein modeling, prediction and analysis. Nat. Protoc. 10, 845–858.
Klaewklad, A., Nakkanong, K., Nathaworn, C.D., Nualsri, C., 2017. Expression of the sucrose transporter 3 (*HbSUT3*) in rubber tree and its relation to latex yield. Mol. Breed. 37, 122.
Koch, K., 2004. Sucrose metabolism: Regulatory mechanisms and pivotal roles in sugar sensing and plant development. Curr. Opin. Plant Biol. 7, 235–246.
Kühn, C., Grof, C.P.L., 2010. Sucrose transporters of higher plants. Curr. Opin. Plant Biol. 13, 288–298.
Kumar, S., Stecher, G., Li, M., Knyaz, C., Tamura, K., 2018. MEGA X: Molecular evolutionary genetics analysis across computing platforms. Mol. Biol. Evol. 35, 1547–1549.
Lalonde, S., Wipf, D., Frommer, W.B., 2004. Transport mechanisms for organic forms of carbon and nitrogen between source and sink. Annu. Rev. Plant Biol. 55, 341–372.
Lalonde, S., Frommer, W.B., 2012. *SUT* Sucrose and *MST* monosaccharide transporter inventory of the Selaginella genome. Front. Plant Sci. 7, 3–24.
Leach, K.A., Tran, T.M., Slewinski, T.L., Meeley, R.B., Braun, D.M., 2017. Sucrose transporter2 contributes to maize growth, development, and crop yield. J. Integr. Plant Biol. 59, 390–408.
Lemoine, R., Bürkle, L., Barker, L., Sakr, S., Kühn, C., Regnacq, M., Gaillard, C., Delrot, S., Frommer, W.B., 1999. Identification of a pollen-specific sucrose transporter-like protein *NtSUT3* from tobacco. FEBS Lett. 454, 325–330.
Lescot, M., Déhais, P., Thijs, G., Marchal, K., Moreau, Y., Van de Peer, Y., Rouzé, P., Rombauts, S., 2002. PlantCARE, a database of plant cis-acting regulatory elements and a portal to tools for in silico analysis of promoter sequences. Nucleic Acids Res. 30, 325–327.
Li, G., Wang, L., Yang, J., He, H., Jin, H., Li, X., Ren, T., Ren, Z., Li, F., Han, X., Zhao, X., Dong, L., Li, Y., Song, Z., Yan, Z., Zheng, N., Shi, C., Wang, Z., Yang, S., Xiong, Z., Zhang, M., Sun, G., Zheng, X., Gou, M., Ji, C., Du, J., Zheng, H., Doležel, J., Deng, X. W., Stein, N., Yang, Q., Zhang, K., Wang, D., 2021. A high-quality genome assembly highlights rye genomic characteristics and agronomically important genes. Nat. Genet. 53, 574–584.
Li, Y., Li, L.L., Fan, R.C., Peng, C.C., Sun, H.L., Zhu, S.Y., Wang, X.F., Zhang, L.Y., Zhang, D.P., 2012. Arabidopsis sucrose transporter *SUT4* interacts with cytochrome b5–2 to regulate seed germination in response to sucrose and glucose. Mol. Plant. 5, 1029–1041.
Li, W., Ren, Z., Wang, Z., Sun, K., Pei, X., Liu, Y., He, K., Zhang, F., Song, C., Zhou, X., Zhang, W., Ma, X., Yang, D., 2018. Evolution and Stress Responses of *Gossypium hirsutum SWEET* Genes. Int. J. Mol. Sci. 19, 769.
Ling, H.Q., Ma, B., Shi, X., Liu, H., Dong, L., Sun, H., Cao, Y., Gao, Q., Zheng, S., Li, Y., Yu, Y., Du, H., Qi, M., Li, Y., Lu, H., Yu, H., Cui, Y., Wang, N., Chen, C., Wu, H., Zhao, Y., Zhang, J., Li, Y., Zhou, W., Zhang, B., Hu, W., van Eijk, M.J.T., Tang, J., Witsenboer, H.M.A., Zhao, S., Li, Z., Zhang, A., Wang, D., Liang, C., 2018. Genome sequence of the progenitor of wheat A subgenome *Triticum urartu*. Nature. 557, 424–428.
Livak, K.J., Schmittgen, T.D., 2001. Analysis of relative gene expression data using real-time quantitative PCR and the 2(-Delta C(T)) Method. Methods. 25 (4), 402–408.
Ma, Q.J., Sun, M.H., Lu, J., Kang, H., You, C.X., Hao, Y.J., 2019. An apple sucrose transporter *MdSUT2.2* is a phosphorylation target for protein kinase *MdCIPK22* in response to drought. Plant Biotechnol. J. 17, 625–637.
Ma, S., Wang, M., Wu, J., Guo, W., Chen, Y., Li, G., Wang, Y., Shi, W., Xia, G., Fu, D., Kang, Z., Ni, F., 2021. WheatOmics: A platform combining multiple omics data to accelerate functional genomics studies in wheat. Mol. Plant. 14, 1965–1968.
Mahboubi, A., Ratke, C., Gorzsás, A., Kumar, M., Mellerowicz, E.J., Niittylä, T., 2013. Aspen SUCROSE TRANSPORTER3 allocates carbon into wood fibers. Plant Physiol. 163, 1729–1740.
Meyer, S., Melzer, M., Truernit, E., Hümmer, C., Besenbeck, R., Stadler, R., Sauer, N., 2000. *AtSUC3*, a gene encoding a new Arabidopsis sucrose transporter, is expressed in cells adjacent to the vascular tissue and in a carpel cell layer. Plant J. 24, 869–882.
Milne, R.J., Byrt, C.S., Patrick, J.W., Grof, C.P., 2013. Are sucrose transporter expression profiles linked with patterns of biomass partitioning in Sorghum phenotypes? Front. Plant Sci. 4, 223.
Nieberl, P., Ehrl, C., Pommerrenig, B., Graus, D., Marten, I., Jung, B., Ludewig, F., Koch, W., Harms, K., Flügge, U.I., Neuhaus, H.E., Hedrich, R., Sauer, N., 2017. Functional characterisation and cell specificity of *BvSUT1*, the transporter that loads sucrose into the phloem of sugar beet (Beta vulgaris L.) source leaves. Plant Biol. (Stuttg.) 19, 315–326.
Niño-González, M., Novo-Uzal, E., Richardson, D.N., Barros, P.M., Duque, P., 2019. More transporters, more substrates: The Arabidopsis major facilitator superfamily revisited. Mol. Plant. 12, 1182–1202.
Oner-Sieben, S., Lohaus, G., 2014. Apoplastic and symplastic phloem loading in Quercus robur and Fraxinus excelsior. J. Exp. Bot. 65, 1905–1916.
Peng, Q., Cai, Y., Lai, E., Nakamura, M., Liao, L., Zheng, B., Ogutu, C., Cherono, S., Han, Y., 2020. The sucrose transporter *MdSUT4.1* participates in the regulation of fruit sugar accumulation in apple. BMC Plant Biol. 20, 191.
Pommerrenig, B., Popko, J., Heilmann, M., Schulmeister, S., Dietel, K., Schmitt, B., Stadler, R., Feussner, I., Sauer, N., 2013. SUCROSE TRANSPORTER 5 supplies Arabidopsis embryos with biotin and affects triacylglycerol accumulation. Plant J. 73, 392–404.
Rees, H., Rusholme-Pilcher, R., Bailey, P., Colmer, J., White, B., Reynolds, C., Ward, S.J., Coombes, B., Graham, C.A., de Barros Dantas, L.L., Dodd, A.N., Hall, A., 2022. Circadian regulation of the transcriptome in a complex polyploid crop. PLoS Biol 20 (10), e3001802.
Reuscher, S., Akiyama, M., Yasuda, T., Makino, H., Aoki, K., Shibata, D., Shiratake, K., 2014. The sugar transporter inventory of tomato: Genome-wide identification and expression analysis. Plant Cell Physiol. 55, 1123–1141.
Riesmeier, J.W., Willmitzer, L., Frommer, W.B., 1994. Evidence for an essential role of the sucrose transporter in phloem loading and assimilate partitioning. EMBO J. 13, 1–7.
Robert, X., Gouet, P., 2014. Deciphering key features in protein structures with the new ENDscript server. Nucleic Acids Res. 42 (W1), W320–W324.
Rottmann, T., Stadler, R., 2019. Measuring sucrose transporter activities using a protoplast-esculin assay. In: Liesche, J. (Ed.), Phloem: Methods and Protocols. Springer, New York, New York, pp. 253–266.
Rottmann, T.M., Fritz, C., Lauter, A., Schneider, S., Fischer, C., Danzberger, N., Dietrich, P., Sauer, N., Stadler, R., 2018. Protoplast-esculin assay as a new method to assay plant sucrose transporters: Characterization of *AtSUC6* and *AtSUC7* sucrose uptake activity in Arabidopsis Col-0 ecotype. Front. Plant Sci. 9, 430.
Ruan, Y.L., 2014. Sucrose metabolism: Gateway to diverse carbon use and sugar signaling. Annu. Rev. Plant Biol. 65, 33–67.
Santiago, J.P., Ward, J.M., Sharkey, T.D., 2020. Phaseolus vulgaris *SUT1.1* is a high affinity sucrose-proton co-transporter. Plant. Direct. 4, e00260.
Shakya, R., Sturm, A., 1998. Characterization of source- and sink-specific sucrose/H+ symporters from carrot. Plant Physiol. 118, 1473–1480.
Slewinski, T.L., Meeley, R., Braun, D.M., 2009. Sucrose transporter1 functions in phloem loading in maize leaves. J. Exp. Bot. 60, 881–892.
Stein, O., Granot, D., 2019. An overview of sucrose synthases in plants. Front. Plant Sci. 10, 95.
Timothy, L., Bailey, J.J., Charles, E.G., William, S.N., 2015. The MEME Suite. Nucl. Acids. Res 43 (W1), W39–W49.
Walkowiak, S., Gao, L., Monat, C., Haberer, G., Kassa, M.T., Brinton, J., Ramirez-Gonzalez, R.H., Kolodziej, M.C., Delorean, E., Thambugala, D., Klymiuk, V., Byrns, B., Gundlach, H., Bandi, V., Siri, J.N., Nilsen, K., Aquino, C., Himmelbach, A., Copetti, D., Ban, T., Venturini, L., Bevan, M., Clavijo, B., Koo, D.H., Ens, J., Wiebe, K., N'Diaye, A., Fritz, A.K., Gutwin, C., Fiebig, A., Fosker, C., Fu, B.X., Accinelli, G.G., Gardner, K.A., Fradgley, N., Gutierrez-Gonzalez, J., Halstead-Nussloch, G., Hatakeyama, M., Koh, C.S., Deek, J., Costamagna, A.C., Fobert, P., Heavens, D., Kanamori, H., Kawaura, K., Kobayashi, F., Krasileva, K., Kuo, T., McKenzie, N., Murata, K., Nabeka, Y., Paape, T., Padmarasu, S., Percival-Alwyn, L., Kagale, S., Scholz, U., Sese, J., Juliana, P., Singh, R., Shimizu-Inatsugi, R., Swarbreck, D., Cockram, J., Budak, H., Tameshige, T., Tanaka, T., Tsuji, H., Wright, J., Wu, J., Steuernagel, B., Small, I., Cloutier, S., Keeble-Gagnère, G., Muehlbauer, G., Tibbets, J., Nasuda, S., Melonek, J., Hucl, P.J., Sharpe, A.G., Clark, M., Legg, E., Bharti, A., Langridge, P., Hall, A., Uauy, C., Mascher, M., Krattinger, S.G., Handa, H., Shimizu, K.K., Distelfeld, A., Chalmers, K., Keller, B., Mayer, K.F.X., Poland, J., Stein, N., McCartney, C.A., Spannagl, M., Wicker, T., Pozniak, C.J., 2020. Multiple wheat genomes reveal global variation in modern breeding. Nature. 588, 277–283.
Wang, D., Liu, H., Wang, H., Zhang, P., Shi, C., 2020. A novel sucrose transporter gene *IbSUT4* involves in plant growth and response to abiotic stress through the ABF-dependent ABA signaling pathway in Sweetpotato. BMC Plant Biol. 20, 157.
Wang, L.F., Qi, X.X., Huang, X.S., Xu, L.L., Jin, C., Wu, J., Zhang, S.L., 2016. Overexpression of sucrose transporter gene *PbSUT2* from Pyrus bretschneideri, enhances sucrose content in Solanum Lycopersicum fruit. Plant Physiol. Biochem. 105, 150–161.
Wang, S., Yang, J., Xie, X., Li, F., Wu, M., Lin, F., Wang, Z., 2019. Genome-wide identification, phylogeny, and expression profile of the sucrose transporter multigene family in tobacco. Can. J. Plant Sci. 99, 312–323.
Wang, Y., Chen, Y., Wei, Q., Wan, H., Sun, C., 2021. Phylogenetic relationships of sucrose transporters (*SUT*s) in plants and genome-wide characterization of *SUT* genes in Orchidaceae reveal roles in floral organ development. PeerJ. 9, e11961.
Xu, Q., Chen, S., Yunjuan, R., Chen, S., Liesche, J., 2018. Regulation of sucrose transporters and phloem loading in response to environmental cues. Plant Physiol. 176, 930–945.

Xu, Q., Yin, S., Ma, Y., Song, M., Song, Y., Mu, S., Li, Y., Liu, X., Ren, Y., Gao, C., Chen, S., Liesche, J., 2020. Carbon export from leaves is controlled via ubiquitination and phosphorylation of sucrose transporter *SUC2*. Proc. Natl Acad. Sci. U. S. A. 117, 6223–6230.

Zhang, H., Liang, W., Yang, X., Luo, X., Jiang, N., Ma, H., Zhang, D., 2010. Carbon starved anther encodes a MYB domain protein that regulates sugar partitioning required for rice pollen development. Plant Cell. 22, 672–689.

Zhao, W., Meng, H., Shi, J., Liu, Y., Yang, Y., Li, L., Wu, C., Wang, L., Wu, G., 2022. Heterologous expression of the peach sucrose transporter (*PpSUT2*) in increased cold and drought stress tolerance in tobacco. J. Hortic. Sci. Biotechnol. 97, 315–327.

Zhu, T., Wang, L., Rimbert, H., Rodriguez, J.C., Deal, K.R., De Oliveira, R., Choulet, F., Keeble-Gagnere, G., Tibbits, J., Rogers, J., Eversole, K., Appels, R., Gu, Y.Q., Mascher, M., Dvorak, J., Luo, M.C., 2021. Optical maps refine the bread wheat *Triticum aestivum* cv. Chinese Spring genome assembly. Plant J. 107 (1), 303–314.